Available online at www.sciencedirect.com
SCIENCE DIRECT®
Remote Sensing of Environment 90 (2004) 337–352
Remote Sensing of Environment
www.elsevier.com/locate/rse

Hyperspectral vegetation indices and novel algorithms for predicting green LAI of crop canopies: Modeling and validation in the context of precision agriculture

Driss Haboudane[a,*], John R. Miller[a,b], Elizabeth Pattey[c], Pablo J. Zarco-Tejada[d], Ian B. Strachan[e]

[a] Centre for Research in Earth and Space Science (CRESS), York University, Petrie Science Building, 4700 Keele St., Toronto, ON, Canada M3J 1P3
[b] Department of Physics and Astronomy, York University, Toronto, ON, Canada M3J 1P3
[c] Agriculture and Agri-Food Canada, Central Experimental Farm, K.W. Neatby Room 2091, 960 Carling Ave., Ottawa, ON, Canada K1A 0C6
[d] Center for Spatial Technologies and Remote Sensing (CSTARS), Department of Land, Air, and Water Resources (LAWR), University of California, Davis, Davis, CA 95616-8671, USA
[e] Department of Natural Resource Sciences, McGill University, 21111 Lakeshore Rd., Ste. Anne de Bellevue, QC, Canada H9X 3V9

Received 4 December 2002; received in revised form 19 December 2003; accepted 29 December 2003

Abstract

A growing number of studies have focused on evaluating spectral indices in terms of their sensitivity to vegetation biophysical parameters, as well as to external factors affecting canopy reflectance. In this context, leaf and canopy radiative transfer models are valuable for modeling and understanding the behavior of such indices. In the present work, PROSPECT and SAILH models have been used to simulate a wide range of crop canopy reflectances in an attempt to study the sensitivity of a set of vegetation indices to green leaf area index (LAI), and to modify some of them in order to enhance their responsivity to LAI variations. The aim of the paper was to present a method for minimizing the effect of leaf chlorophyll content on the prediction of green LAI, and to develop new algorithms that adequately predict the LAI of crop canopies. Analyses based on both simulated and real hyperspectral data were carried out to compare performances of existing vegetation indices (Normalized Difference Vegetation Index [NDVI], Renormalized Difference Vegetation Index [RDVI], Modified Simple Ratio [MSR], Soil-Adjusted Vegetation Index [SAVI], Soil and Atmospherically Resistant Vegetation Index [SARVI], MSAVI, Triangular Vegetation Index [TVI], and Modified Chlorophyll Absorption Ratio Index [MCARI]) and to design new ones (MTVI1, MCARI1, MTVI2, and MCARI2) that are both less sensitive to chlorophyll content variations and linearly related to green LAI. Thorough analyses showed that the above existing vegetation indices were either sensitive to chlorophyll concentration changes or affected by saturation at high LAI levels. Conversely, two of the spectral indices developed as a part of this study, a modified triangular vegetation index (MTVI2) and a modified chlorophyll absorption ratio index (MCARI2), proved to be the best predictors of green LAI. Related predictive algorithms were tested on CASI (Compact Airborne Spectrographic Imager) hyperspectral images and, then, validated using ground truth measurements. The latter were collected simultaneously with image acquisition for different crop types (soybean, corn, and wheat), at different growth stages, and under various fertilization treatments. Prediction power analysis of proposed algorithms based on MCARI2 and MTVI2 resulted in agreements between modeled and ground measurement of non-destructive LAI, with coefficients of determination (r^2) being 0.98 for soybean, 0.89 for corn, and 0.74 for wheat. The corresponding RMSE for LAI were estimated at 0.28, 0.46, and 0.85, respectively.

Keywords: Hyperspectral; Spectral indices; Green LAI; Prediction algorithms; Chlorophyll content; Precision agriculture

1. Introduction

Green leaf area index (LAI) is a key variable used by crop physiologists and modelers for estimating foliage cover, as well as forecasting crop growth and yield. Its determination is critical for understanding biophysical processes of forest and crop canopies and for predicting their growth and productivity (Daughtry et al., 1992; Goetz & Prince, 1996; Liu et al., 1997; Moran et al., 1995, 1997; Tucker et al., 1980). The expression "green LAI", used in this paper, represents the LAI of living leaves regardless to their photosynthetic capacity. Living leaves can have similar structural characteristics but various pigment contents (i.e.,

* Corresponding author. Fax: +1-416-736-5626.
E-mail address: driss@terra.phys.yorku.ca (D. Haboudane).

0034-4257/$ - see front matter © 2004 Elsevier Inc. All rights reserved.
doi:10.1016/j.rse.2003.12.013

chlorophyll). The exposed area of living leaves plays a key role in various biophysical processes such as plant transpiration and CO_2 exchange. These functions are important for understanding exchanges between the vegetation and the atmosphere. Because LAI is functionally linked to the canopy spectral reflectance, its retrieval from remote sensing data has prompted many investigations and studies in recent years. This has led to the development of different techniques aiming to improve its estimation over large areas, mainly through the use of spectral indices, model inversions, and spectral mixture analysis. The latter has been successfully used to define an end-member of interest, determine its relative abundance, then correlate it with ground-measured LAI; thus, more or less significant correlation levels were found between LAI and sunlit fraction (Hu et al., 2004), shadow fraction (Peddle & Johnson, 2000), and crop fraction (Pacheco et al., 2001). Only very few studies have focused on inversion of sophisticated radiative transfer models to retrieve green LAI of crop canopies (Jacquemoud et al., 2000). The common and widely used approach has been to develop relationships between ground-measured LAI and vegetation indices (Chen & Cihlar, 1996; Fassnacht et al., 1997; Spanner et al., 1990). Consequently, a large number of relationships have been established, and a wide range of determination coefficients ($0.05 < r^2 < 0.66$) between satellite-derived spectral indices and LAI were found (Baret & Guyot, 1991; Brown et al., 2000; Chen, 1996).

During recent decades, substantial efforts were expended in improving the Normalized Difference Vegetation Index (NDVI) and in developing new indices aiming to compensate for soil background influences (Bannari et al., 1996; Baret et al., 1989; Huete, 1988; Qi et al., 1994; Rondeaux et al., 1996), as well as for atmospheric effects (Karnieli et al., 2001; Kaufman & Tanre, 1992). Even though the external perturbing factors related to changes in soil brightness and atmospheric conditions were taken into account, vegetation indices still have definite intrinsic limitations; they are not a single measure of a specific variable of interest such as pigment content, plant geometry, or canopy architecture. So far, it has not been possible to design an index which is sensitive only to the desired variable and totally insensitive to all other vegetation parameters (Govaerts et al., 1999). Therefore, different indices were defined for different purposes, and optimized to assess a process of interest. For instance, some spectral indices were proposed to capture the photochemical processes associated with photosynthesis activity such as light use efficiency or to estimate leaf pigment content (Broge & Leblanc, 2000; Chappelle et al., 1992; Daughtry et al., 2000; Gamon et al., 1992; Haboudane et al., 2002; Kim et al., 1994). Others were designed to retrieve LAI (Brown et al., 2000; Chen, 1996) or to quantify vegetation fraction (Gitelson et al., 2001).

A major problem in the use of these indices arises from the fact that canopy reflectance, in the visible and near-infrared, is strongly dependent on both structural (e.g., LAI) and biochemical properties (e.g., chlorophyll) of the canopy (Goel, 1988; Jacquemoud et al., 2000; Zarco-Tejada et al., 2001). Moreover, LAI and chlorophyll content have similar effects on canopy reflectance particularly in the spectral region from the green (550 nm) to the red edge (750 nm). To uncouple their combined effect, recent studies (Daughtry et al., 2000; Haboudane et al., 2002) have demonstrated that leaf chlorophyll content can be estimated with minimal confounding effects due to LAI through a combination of two kinds of spectral indices: indices sensitive to pigment concentration and indices resistant to soil optical properties influence. Conversely, no studies have focused on the retrieval of LAI without interference of chlorophyll effects. The latter generate a considerable scatter in the relationship between LAI and the vegetation index of choice.

In practice, LAI prediction from remotely sensed data faces two major difficulties: (1) vegetation indices approach a saturation level asymptotically when LAI exceeds 2 to 5, depending on the type of vegetation index; (2) there is no unique relationship between LAI and a vegetation index of choice, but rather a family of relationships, each a function of chlorophyll content and/or other canopy characteristics. To address these issues, a few studies have been carried out to assess and compare various vegetation indices in terms of their stability and their prediction power of LAI (Baret & Guyot, 1991; Broge & Leblanc, 2000) while others have dealt with modifying some vegetation indices to improve their linearity with, and increase their sensitivity to, LAI (Chen, 1996; Brown et al., 2000; Nemani et al., 1993). Consequently, some indices have been identified as best estimators of LAI because they are less sensitive to the variation of external parameters affecting the spectral reflectance of the canopy, namely soil optical properties, illumination geometry, and atmospheric conditions. However, the effect of leaf chlorophyll variations on the LAI–vegetation index relationship remains an unsolved problem. How does chlorophyll concentration influence the behavior of a vegetation index of choice? Which of these indices, suitable to LAI prediction, is least sensitive to chlorophyll changes? Is there a single LAI versus vegetation index curve for a wide range of leaf chlorophyll content?

The need for an answer to these questions has inspired the present study as a contribution to improving the use of hyperspectral remote sensing to predict LAI in the context of precision farming. The main purpose is to suggest a spectral index that is suitable to simply, and yet accurately, determine LAI of crop canopies for agriculture management purposes. The research focuses on reducing the variability in LAI estimates due to changes in leaf chlorophyll concentration. To achieve these objectives, PROSPECT and SAILH radiative transfer models were used to simulate crop canopy reflectance for various biochemical, structural and observation conditions, then a set of indices that have proven to be resistant to atmospheric and soil brightness effects were assessed in terms of their responsivity/resistance to chlorophyll content variability. Another objective

was to validate the modeling approach through the application to airborne hyperspectral data and the comparison with field measurements carried out simultaneously with image acquisition.

2. Methods

2.1. The study area

The study area is located at the former Greenbelt Farm of Agriculture and Agri-Food Canada (45°18′ N, 75°45′ W, Ottawa, Canada). Over three successive years, different crops (corn, wheat, soybean) were grown on a 30-ha field with a drained clay loam soil as well as on adjacent fields managed by private producers. Prior knowledge of the field management and plant stress patterns helped in selecting ground truth sites of contrasting productivity in order to test the performance of predictive algorithms developed through modeling and scaling up approaches, and to validate the results of the algorithms' application to CASI airborne hyperspectral images. The sites were thus located to promote the development of remote sensing techniques for detection of plant stresses (particularly nitrogen deficiency, water deficit and low organic matter in the soil root zone) in precision agriculture. Details on the field in situ instrumentation and measuring approaches are presented in Pattey et al. (2001) and in Strachan et al. (2002).

2.2. Airborne and field data

Hyperspectral images were acquired by the Compact Airborne Spectrographic Imager (CASI, Calgary, Canada), flown by the Centre for Research in Earth and Space Technology (CRESTech). At the same time, a comprehensive field and laboratory database was assembled which included measurements of leaf reflectance and transmittance measurements using an integrating sphere (Li-Cor model 1800-12, Lincoln, NE) coupled by a single mode optic fibre to a spectrometer (GER1500, GER, Millbrook, NY), and leaf area index (LAI) using the Plant Canopy Analyzer (LAI-2000; Li-Cor) set for quantifying non-destructive total LAI and an area meter (LI-3100, Li-Cor) for determining separately destructive LAI of green and dead leaves. The destructive leaf area measurements were used to calculate the proportion of green LAI. Non-destructive LAI measurements were then multiplied by green leaf area proportion to calculate green LAI on a wider spatial area basis.

During the 2000 and 2001 growing seasons, CASI hyperspectral images were collected in three different deployments, using two modes of operation: the *multispectral mode*, with 1-m spatial resolution and 7 spectral bands suitable for sensing vegetation properties (489.51, 554.98, 624.63, 681.42, 706.12, 742.31, and 776.69 nm); and the *hyperspectral mode*, with 2-m spatial resolution and 72 channels covering the visible and near infrared portions of the solar spectrum from 408 to 947 nm with a bandwidth of 7.5 nm. Acquisition dates were planned to coincide with different phenological development stages, providing image data covering the early vegetative, active growth and reproductive periods of each growing season. In this study we used four images acquired in 2000, and three images acquired in 2001. In 1999, only one hyperspectral image was acquired on August 23rd.

2.3. CASI hyperspectral data processing

The processing of CASI imagery included the following separate stages: raw data to radiance transformation, atmospheric corrections and reflectance retrieval, removal of aircraft motion effects and geo-referencing, and flat field adjustments of surface reflectance spectra.

The hyperspectral digital images collected by CASI were processed to at-sensor radiance using calibration coefficients determined in the laboratory by CRESTech. The CAM5S atmospheric correction model (O'Neill et al., 1997) was then used to transform the relative at-sensor radiance to absolute ground-reflectance. To perform this operation, an estimate of aerosol optical depth at 550 nm was derived from ground sun-photometer measurements. Reflectance spectra of asphalt and concrete within CASI imagery were used to calculate coefficients that adequately compensate for residual effects of atmospheric water and oxygen absorption, and therefore to perform the flat field calibration. Data regarding geographic position, illumination and viewing geometry as well as ground and sensor altitudes were derived both from aircraft navigation data recordings and ground DGPS measurements.

2.4. Crop canopy reflectance simulations

Leaf optical properties were simulated using the PROSPECT model (Jacquemoud & Baret, 1990; Jacquemoud et al., 1996), which simulates upward and downward hemispherical radiation fluxes between 400 and 2500 nm, and relates foliar biochemistry and scattering parameters to leaf reflectance and transmittance spectra. It requires the leaf internal structure parameter N, the chlorophyll a + b content C_{ab} (μg cm^{-2}), the equivalent water thickness C_w (cm), and the leaf dry matter content C_m (g cm^{-2}) to determine leaf reflectance and transmittance signatures in the optical domain.

Input parameters C_w and C_m were assigned the nominal values of 0.0015 cm and 0.0035 g cm^{-2}, respectively. The parameter N has been estimated by inverting the PROSPECT model on corn reflectance and transmittance spectra measured in the laboratory using an integrating sphere coupled to a spectrometer. The mean value 1.41 was thereby obtained, and is in agreement with the value ($N = 1.4$) used for corn plants by Jacquemoud et al. (2000). We have also used $N = 1.55$ as an average value for various crops, including corn, soybean, and wheat. With these inputs,

reflectance and transmittance spectra were generated for chlorophyll content varying from 5 to 100 μg cm^{-2} for the purpose of simulating corn canopy reflectance (SAILH model) for a wide range of chlorophyll concentrations.

Canopy reflectance spectra were simulated using a variant of the SAIL (Scattering by Arbitrary Inclined Leaves) model (Verhoef, 1984) called SAILH. It was adapted to take into account the hotspot effect or the multiple scattering in the canopy (Kuusk, 1985). It is a turbid-medium model that approximates the canopy as a horizontally uniform parallel-plane infinitely extended medium, with diffusely reflecting and transmitting elements. Discussions and mathematical formalisms of SAIL and SAILH are provided by Goel (1988, 1989), Verhoef (1984, 1998), and Zarco-Tejada (2000). Typical SAILH inputs are (Table 1): canopy architecture defined by the leaf area index (LAI) and the leaf angle distribution function (LADF), leaf reflectance and transmittance spectra for given chlorophyll content per unit area, underlying soil reflectance, and the illumination and viewing geometry (solar zenith and sensor viewing angles).

2.5. Spectral vegetation indices selected for this research

Several optical indices have been reported in the literature and have been proven to be well correlated with various vegetation parameters such as LAI, biomass, chlorophyll concentration, photosynthetic activity, and more. Exhaustive comparative studies have been already carried out to assess the prediction power of different optical indices and their sensitivity to various canopy parameters and external factors (e.g., Bannari et al., 1995; Baret & Guyot, 1991; Broge & Leblanc, 2000; Chen, 1996; Karnieli et al., 2001; Zarco-Tejada, 2000). Much effort has been expended to improve vegetation indices and render them insensitive to variations in illumination conditions, observing geometry, and soil properties. Thus, the performance and the suitability of a particular index are generally determined by the sensitivity of the index to a characteristic of interest. For this reason, and based on the conclusions of the above-mentioned studies, indices specifically designed to detect leaf pigments, vegetation stress, or vegetation fraction will not be considered in this study. Rather, a few of the most common vegetation indices were selected and regrouped into three categories according to their formalism and their adherence to the same family.

Table 1
Input variables for SAILH model

SAILH input variables	Description/values
Leaf optical properties	Simulated reflectance and transmittance (PROSPECT) for various chlorophyll content, from 5 to 1000 μg cm^{-2}, in 5 μg cm^{-2} steps
Soil reflectance	Reflectance spectrum of a developed soil (400–2400 nm)
Leaf area index	0.1, 0.3, 0.5, 1, 1.5, 2, 2.5, 3, 4, 5, 6, 7, 8, 9, 10, 11, 12
Lead angle distribution function (LADF)	Spherical
Sun zenith angle	35° and 45°
Sensor viewing angle	0° (nadir)
Fraction of direct coming radiation	1

2.6. Indices based on the normalized difference: improving the linearity

The most known and widely used vegetation index is the Normalized Difference Vegetation Index (NDVI) developed by Rouse et al. (1974). It is based on the contrast between the maximum absorption in the red due to chlorophyll pigments and the maximum reflection in the infrared caused by leaf cellular structure. Using hyperspectral narrow bands, this index is quantified by the following equation where R_x is the reflectance at the given wavelength (nm):

$$\mathrm{NDVI} = (R_{800} - R_{670})/(R_{800} + R_{670}) \quad (1)$$

Despite its intensive use, NDVI saturates in cases of dense and multi-layered canopy and shows a non-linear relationship with biophysical parameters such as green LAI (Baret & Guyot, 1991; Lillesaeter, 1982). Therefore, improved indices like the Renormalized Difference Vegetation Index (RDVI; Rougean & Breon, 1995) and the Modified Simple Ratio (MSR; Chen, 1996) have been developed in order to linearize their relationships with vegetation biophysical variables. The RDVI (Eq. (2)) was proposed to combine the advantages of the Difference Vegetation Index (DVI = NIR − Red; Jordan, 1969) and the NDVI for low and high LAI values, respectively.

$$\mathrm{RDVI} = (R_{800} - R_{670})/\sqrt{(R_{800} + R_{670})} \quad (2)$$

MSR (Eq. (3)) was suggested as an improvement over RDVI in terms of sensitivity to vegetation biophysical parameters through its combination with the Simple Ratio (SR = NIR/Red; Jordan, 1969). SR and MSR are considered more linearly related to vegetation parameters:

$$\mathrm{MSR} = \left(\frac{R_{800}}{R_{670}} - 1\right) \Big/ \sqrt{\left(\frac{R_{800}}{R_{670}} + 1\right)} \quad (3)$$

2.7. Soil–line vegetation indices: improving the resistance to soil and atmospheric effects

To account for changes in the soil optical properties, soil-adjusted indices minimizing the background influence have been developed. The leading index in such improvement is the Soil-Adjusted Vegetation Index (SAVI; Huete, 1988),

which includes a canopy background adjustment factor L. Using narrow bands, SAVI is formulated as:

$$\mathrm{SAVI} = (1+L)(R_{800}-R_{670})/(R_{800}+R_{670}+L) \quad (4)$$

The factor L is a function of vegetation density, and its determination requires a prior knowledge of vegetation amounts (Huete, 1988). The value of factor L is critical in the minimization of soil optical properties effects on vegetation reflectance. Huete (1988) suggested an optimal value of $L=0.5$ to account for first-order soil background variations. Attempting to improve SAVI with regard to the differences in soil background, Qi et al. (1994) developed an improved SAVI (MSAVI) with a self-adjustment factor L that does not appear in the formulation of MSAVI. Using hyperspectral bands, MSAVI is calculated as:

$$\mathrm{MSAVI} = \frac{1}{2}\left[2R_{800}+1-\sqrt{(2R_{800}+1)^2-8(R_{800}-R_{670})}\right] \quad (5)$$

A recent study by Broge and Leblanc (2000) using radiative transfer models has found that MSAVI is the best LAI estimator in terms of sensitivity to canopy effects. It proved to be less affected by variations in canopy parameters as well as soil spectral properties. Furthermore, it was the best LAI estimator in dense canopies.

To minimize atmospheric-induced variations in NDVI, Kaufman and Tanre (1992) have corrected the red radiance for aerosol effect by incorporating the blue channel. The corrected red channel is obtained using the following formula where subscripts r and b denote the red and blue bands, respectively:

$$R_{\mathrm{rb}} = R_{\mathrm{r}} - \gamma(R_{\mathrm{b}}-R_{\mathrm{r}}) \quad (6)$$

The authors recommend a value of 1 for the function γ. This led to the development of the Soil and Atmospherically Resistant Vegetation Index (SARVI), which minimizes both canopy background and atmospheric effects (Kaufman & Tanre, 1992):

$$\mathrm{SARVI} = (1+L)(R_{800}-R_{\mathrm{rb}})/(R_{800}+R_{\mathrm{rb}}+L) \quad (7)$$

2.8. New vegetation indices based on three discrete bands

Indices incorporating bands in the green and red-edge parts of the solar spectrum were developed to measure the light absorption by chlorophyll in the red region (670 nm). Kim et al. (1994) introduced the ratio (R_{700}/R_{670}) to minimize the combined effects of the underlying soil reflectance and the canopy non-photosynthetic materials, while Gitelson and Merzlyak (1996) have found a strong correlation between leaf chlorophyll concentration and the reflectance ratios (R_{750}/R_{550}) and (R_{750}/R_{700}).

Kim et al. (1994) developed the Chlorophyll Absorption Ratio Index (CARI) which measures the depth of chlorophyll absorption at 670 nm relative to the green reflectance peak at 550 nm and the reflectance 700 nm. The CARI was, then, simplified by Daughtry et al. (2000) to obtain the Modified Chlorophyll Absorption Ratio Index (MCARI), which is quantified by the following equation:

$$\mathrm{MCARI} = [(R_{700}-R_{670})-0.2(R_{700}-R_{550})](R_{700}/R_{670}) \quad (8)$$

Even though MCARI was developed to be responsive to chlorophyll variation in the first place, Daughtry et al. (2000) found that LAI, chlorophyll, and chlorophyll–LAI interaction accounted, respectively, for 60%, 27%, and 13% of MCARI variation. Therefore, MCARI holds a great potential for LAI predictions albeit no near-infrared band (or wavelength) was considered in its formulation.

Inspired by the general idea of CARI, Broge and Leblanc (2000) developed the Triangular Vegetation Index (TVI), which is meant to characterize the radiant energy absorbed by leaf pigments in terms of the relative difference between red and near-infrared reflectance in conjunction with the magnitude of reflectance in the green region. TVI is determined as the area defined by the green peak, the near-infrared shoulder, and the minimum reflectance in the red region. It is formulated as:

$$\mathrm{TVI} = 0.5[120(R_{750}-R_{550})-200(R_{670}-R_{550})] \quad (9)$$

The general idea behind TVI is based on the fact that the total area of the triangle (green, red, infrared) will increase as a result of chlorophyll absorption (decrease of red reflectance) and leaf tissue abundance (increase of near-infrared reflectance) (Broge & Leblanc, 2000). While this remains true, it is important to notice that the increase of chlorophyll concentration also results in the decrease of the green reflectance, leading, therefore, to a relative decrease of the triangle area. Furthermore, although there is no chlorophyll absorption beyond 700 nm, chlorophyll indirect effects on the vegetation reflectance curve remain observable around the red edge position up to 750 nm. In fact, as chlorophyll content increases, its absorption feature broadens and causes the red-shift of the red-edge reflectances. Consequently, the canopy reflectance at 750 nm is still influenced by leaf chlorophyll content.

2.9. Improved new vegetation indices for green LAI predictions

As a part of this study, we developed modified versions of these new indices that are suitable to LAI estimation from remote sensing data. The general idea behind these modifications was to render these indices (MCARI and TVI) less sensitive to chlorophyll effects, more responsive to green LAI variations, and more resistant to soil and atmosphere effects.

For this reason, we suggest the introduction of two main changes to MCARI: the suppression of the ratio (R_{700}/R_{670}) in order to lower the sensitivity to chlorophyll effects, and the integration of a near-infrared wavelength to increase the sensitivity to LAI changes. Consequently, Eq. (8) is simplified, and a variant of MCARI is obtained and denoted MCARI1. It is formulated as

$$\mathrm{MCARI1} = 1.2[2.5(R_{800} - R_{670}) - 1.3(R_{800} - R_{550})] \quad (10)$$

Regarding TVI, the transformation is based on the fact that the increase of the chlorophyll concentration causes a red-shift of red-edge reflectances, introducing changes to reflectance at 750 nm which represents the beginning of the infrared shoulder. To make TVI suitable for LAI estimations, the 750 nm wavelength was replaced by the 800 nm wavelength, the reflectance of which is influenced by the changes in leaf and canopy structures, and is insensitive to pigment level changes. Applying a scale factor, we defined a modified TVI (denoted MTVI1) according to:

$$\mathrm{MTVI1} = 1.2[1.2(R_{800} - R_{550}) - 2.5(R_{670} - R_{550})] \quad (11)$$

To reduce soil contamination effects, we incorporated a soil adjustment factor, using the concept developed by Huete (1988). This term was optimized with the constraint of preserving the sensitivity to LAI as well as the resistance to chlorophyll influence. Consequently, improved versions of MCARI and TVI were formulated as:

$$\mathrm{MCARI2} = \frac{1.5[2.5(R_{800} - R_{670}) - 1.3(R_{800} - R_{550})]}{\sqrt{(2R_{800}+1)^2 - (6R_{800} - 5\sqrt{R_{670}}) - 0.5}} \quad (12)$$

$$\mathrm{MTVI2} = \frac{1.5[1.2(R_{800} - R_{550}) - 2.5(R_{670} - R_{550})]}{\sqrt{(2R_{800}+1)^2 - (6R_{800} - 5\sqrt{R_{670}}) - 0.5}} \quad (13)$$

These two indices were used to determine green LAI predicting functions, which were based on simulations with PROSPECT and SAILH radiative transfer models, as well as on an optical-index scaling-up approach discussed in detail in Zarco-Tejada et al. (2001). Performances of all the indices presented in this section, as well as results of the proposed approach are presented, discussed and compared to ground truth measurements in the following section.

3. Results and analysis

3.1. Sensitivity to chlorophyll effects and saturation level: simulated data

The relationships between vegetation indices and green LAI are not unique, they exhibit a considerable scatter caused by chlorophyll content variation and/or the influence of other canopy characteristics. In fact, the indices are designed to measure vegetation greenness in which chlorophyll content plays a major role beside the amount of green leaves. To understand this influence, vegetation indices selected for this study are plotted against green LAI as a function of chlorophyll concentrations (Figs. 1 and 2); the curves represent chlorophyll content varying from 20 to 100μg cm^{-2} with an increment of 5 μg cm^{-2}. In these figures, scaling factors were applied to MSR and TVI in order to have their values scaled between 0 and 1 for comparison with other indices. As can be seen, all indices behave logarithmically rather than linearly with LAI.

MCARI and MSR are the most affected by chlorophyll variability, showing high sensitivity even at high chlorophyll levels (up to 60 μg cm^{-2}). This can be explained by the integration in their formulae of ratios that are highly correlated to leaf and canopy chlorophyll content: (R_{700}/R_{670}) and (R_{800}/R_{670}), respectively. Such a behavior is expected, in the case of MCARI, which was designed to measure the chlorophyll influence in the red and red-edge regions, but is intriguing in the case of MSR, which is defined to estimate LAI in forest landscapes. Moreover, MSR is meant to improve the linearity and overcome the saturation limits of RDVI. This is true, but only at high levels of canopy chlorophyll content (Fig. 1), which is generally more applicable to forestry than to agriculture.

MSAVI and NDVI exhibit a similar resistance to chlorophyll content variability, with clear sensitivity only at to low and low-medium chlorophyll concentrations (less than 35 μg cm^{-2}). The main difference between these two indices resides in the saturation effect when LAI increases: NDVI reaches a saturation level asymptotically when LAI exceeds 2, while MSAVI shows a better trend without a clear saturation at high LAI levels (up to 6) (Fig. 1). This explains, in part, why MSAVI has proven to be a better indicator of greenness measure (Broge & Leblanc, 2000).

Indices RDVI, SAVI, and SARVI show a very similar behavior in many regards. They are less sensitive to chlorophyll content than both NDVI and MSAVI, they have a relatively limited dynamic (values comprised between 0.05 and 0.75), and they are less affected by saturation than NDVI, but more than MSAVI. Despite their relative insensitivity to low chlorophyll effects, these indices are not good for characterization of greenness of dense canopies with high LAI (LAI>4) (Fig. 1).

The Triangular Vegetation Index (TVI) seems to be a good candidate for green LAI estimations, but its sensitivity to chlorophyll content increases with the increase of canopy density as illustrated by Fig. 1 (LAI>4). This finding is based on the concept behind the TVI itself (triangle area) and the use of the wavelength 750 nm. In fact, the increase of chlorophyll concentration causes the increase of the triangle area, and at the same time it moves the near-infrared shoulder to longer wavelengths (higher than 750 nm). Therefore, beyond a certain level of canopy development,

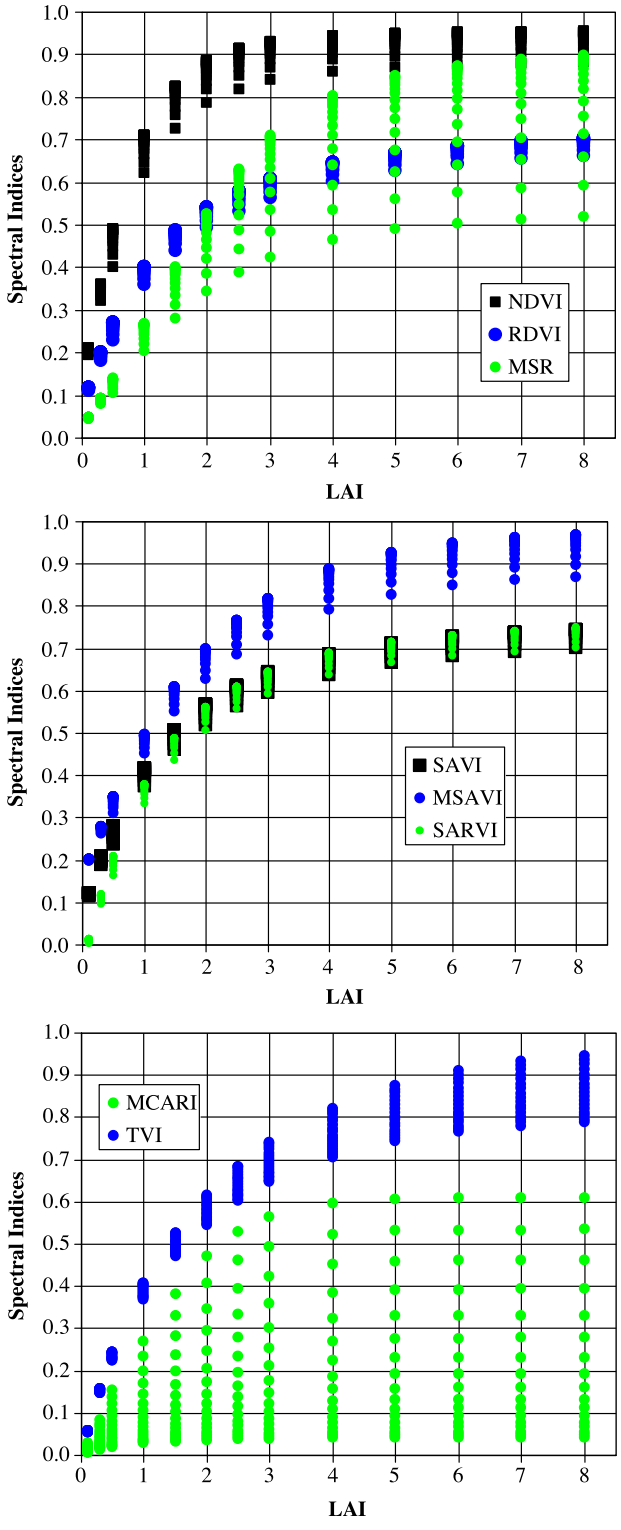

Fig. 1. Effects of chlorophyll concentration variation on the relationships between vegetation indices and green leaf area index (LAI). Application to canopy reflectance simulated using PROSPECT and SAILH. The curves correspond to various chlorophyll concentrations ranging from 20 to 100 μg cm^{-2} with steps of 5 μg cm^{-2}. For clarity purposes, MSAVI was scaled up by adding 0.1.

the use of 750 nm does not capture variations due only to LAI, and triangle area changes are mainly controlled by variations in chlorophyll concentration.

The best behavior in terms of both resistance to pigments variation and responsiveness to LAI changes is given by the improved indices MTVI1 and MCARI1 (Fig. 2). They offer the advantage of being more or less resistant to chlorophyll changes and the least sensitive to the saturation phenomena. Indeed, MTVI1 and MCARI1 can have a unique relationship with green LAI, with almost no significant influence of chlorophyll changes between 20 and 100 μg cm^{-2} (Fig. 2). Their counterparts, MTVI2 and MCARI2, lead to similar performances with a slight difference in the dynamic at high LAI values. MTVI2 and MCARI2 show a similar behavior as MSAVI, but have the advantage of being less sensitive to chlorophyll concentration changes.

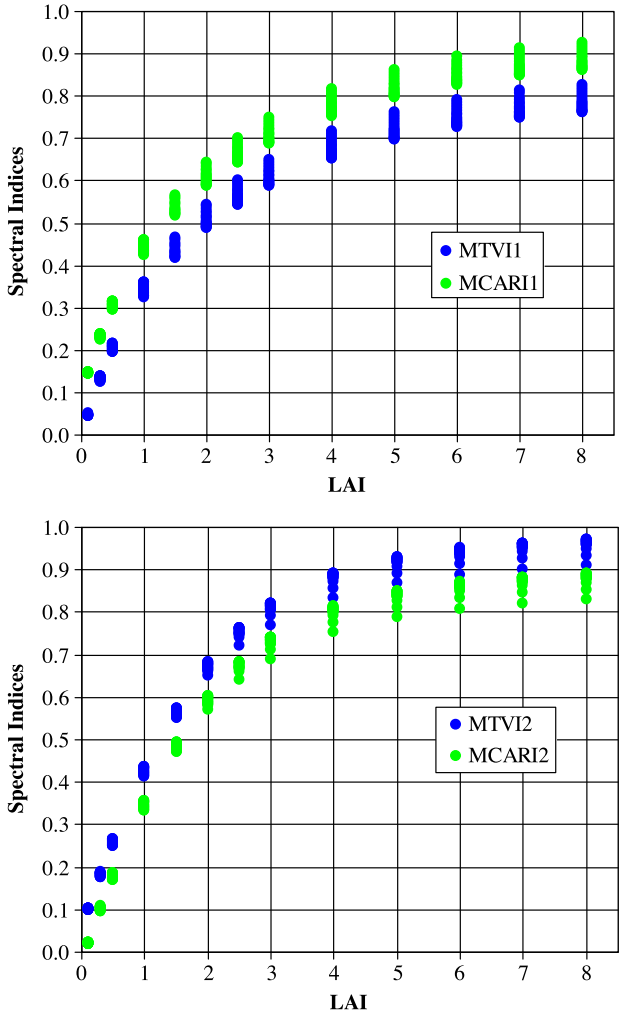

Fig. 2. Relationships between the modified vegetation indices (MTVI1, MCARI1, MTVI2, and MCARI2) and green leaf area index (LAI). Application to canopy reflectance simulated using PROSPECT and SAILH. The curves correspond to various chlorophyll concentrations ranging from 20 to 100 μg cm^{-2} with a step of 5 μg cm^{-2}. For clarity purposes, MCARI1 and MTVI2 were scaled up by adding 0.1 and 0.08, respectively.

3.2. Linearity analysis: real CASI hyperspectral data

To assess differences in vegetation indices behavior, we extracted spectral reflectance signatures from CASI hyperspectral images collected during summers of 1999, 2000, and 2001, over agricultural fields with three crop types: corn, wheat, and soybean. We then plotted the indices against the near-infrared (NIR) reflectance (Fig. 3) in order to compare each index's ability to depict green LAI variations. For comparison clarity, some indices are plotted in more than one scatterplot. The rationale for this analysis was that the NIR reflectance is strongly affected by changes in vegetation structural descriptors rather than by pigment variation. In fact, while visible bands (namely red) are sensitive to soil background effects, the NIR offers the best discrimination of vegetation structural variations.

Distinct behaviors were clearly identifiable in Fig. 3 with respect to the increase of NIR reflectance. As expected, NDVI showed the weakest correlation with NIR reflectance, and became saturated at approximately 0.91 when NIR increased from 0.35 to 0.80. It showed little sensitivity to the variations in green vegetation density. MSR exhibited a similar behavior, which is coupled with a considerable scatter in the relationship MSR–NIR. Indeed, MSR saturated for NIR values ranging from 0.45 to 0.80, and presented a substantial dispersion of its values due to its sensitivity to the red reflectances. To explain this performance, we used the same CASI hyperspectral dataset to plot various NIR–Red combinations as a function of NIR reflectance (Fig. 4). We found that the addition (NIR + Red) and subtraction (NIR – Red) were linearly and strongly correlated to NIR reflectance changes, while the product (NIR∗Red) and the ratio (NIR/Red) exhibited a positive correlation but a very scattered relationship with NIR reflectance. It is important to mention that the product and the ratio were scaled for comparison purposes (Fig. 4). Consequently, indices using the ratio or the product of NIR and Red wavelengths are very sensitive to chlorophyll content variations, and are not good estimates of green LAI dynamics.

In contrast with NDVI and MSR, indices RDVI, SAVI, MSAVI, and SARVI behaved quite differently (Fig. 3); they appeared to be much more responsive to NIR reflectance changes. Nevertheless, their linear relationship with NIR reflectance is characterized by a slope change around NIR = 0.45. They increased substantially with the increase of NIR, then followed a slight asymptotic trend at higher NIR values. Although MSAVI exhibited some scattering, it provided the best performance of its group, with a better dynamic (best average slope) for NIR values ranging from 0.23 to 0.60. This is consistent with the findings of Broge and Leblanc (2000) who concluded that MSAVI was the best LAI estimator in dense canopies.

Overall, the best linear relationship between NIR reflectance and vegetation indices is offered by the indices MTVI1, MCARI1, MTVI2, and MCARI2. They showed clear linear relationships without a pronounced change of the slope, as well as no asymptotic trend at higher NIR reflectance values (Fig. 3). However, MTVI1 and MCARI1

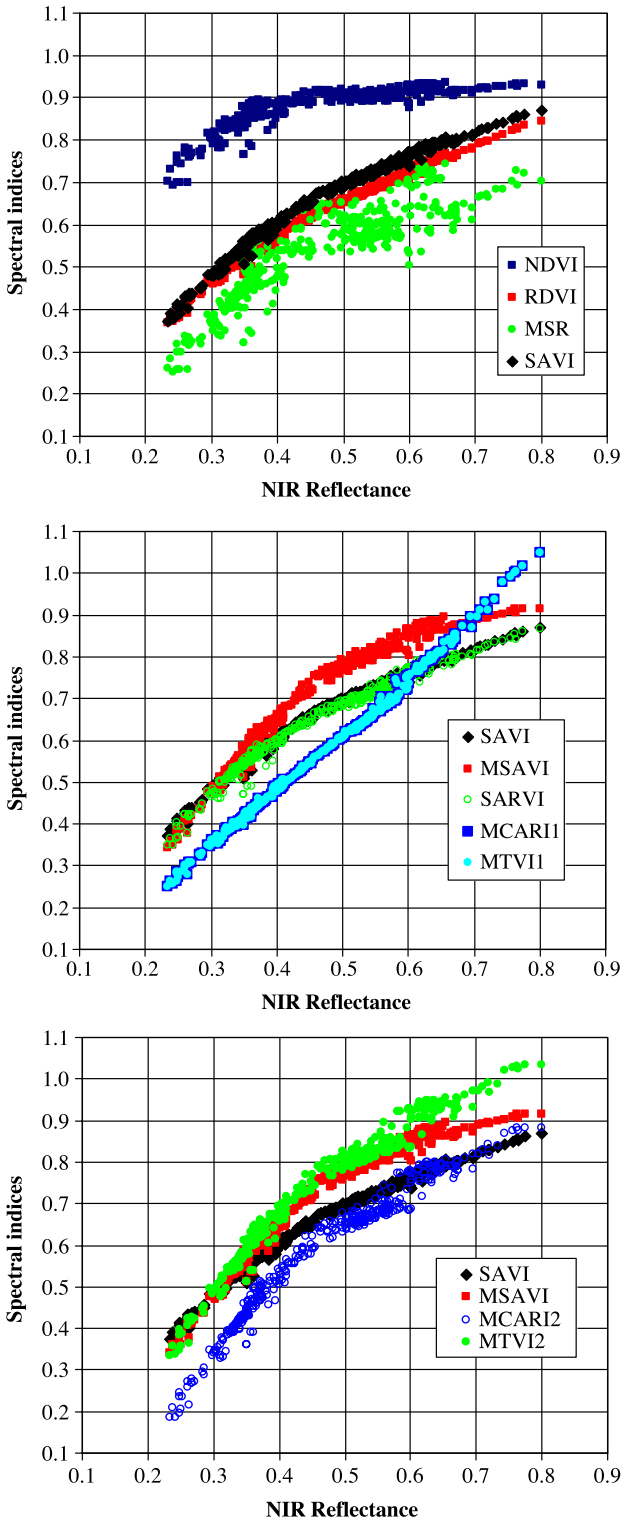

Fig. 3. Relationships between the evaluated spectral indices and the near-infrared (NIR) reflectance from CASI hyperspectral images collected over different crops (corn, wheat, and soybean). For clarity purposes, MCARI2 was scaled down by subtracting 0.15.

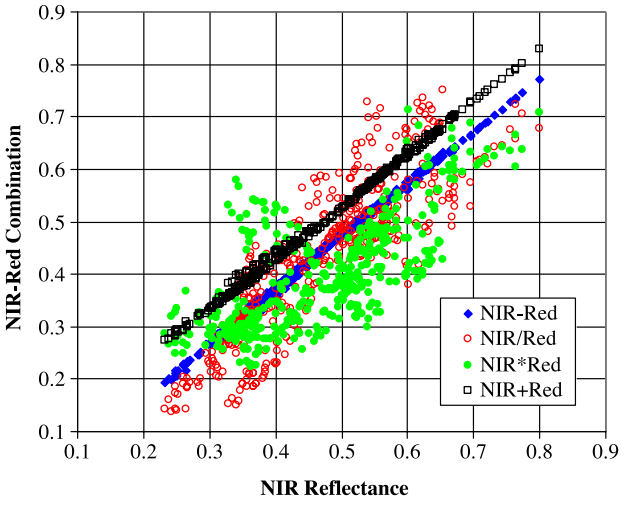

Fig. 4. Relationships between the near-infrared (NIR) reflectance and Red–NIR combinations, from CASI hyperspectral images collected over different crops (corn, wheat, and soybean). For clarity purposes, NIR/Red and NIR∗Red were multiplied by factors of 0.025 and 30, respectively.

are strongly coupled with NIR reflectances, providing the best overall dynamic with a constant slope for the whole range of NIR reflectance. This behavior is due to the formalism of these indices which use only a combination of waveband differences. Indeed, as can be seen in Fig. 5, the difference (NIR – Green) is strongly correlated with canopy NIR reflectance. Conversely, the difference (Green – Red) is not linearly related to the NIR reflectance, but it is important to notice that its low values are dominated by those of the difference (NIR – Green) in the calculation of MTVI variants.

3.3. Green LAI estimation: predictive functions

To estimate LAI from remotely sensed data, empirical relationships between LAI and spectral indices were proposed. Equations describing these relationships vary in both mathematical forms (linear, exponential, power, inverse of exponential, etc.) and empirical coefficients, depending on the experiments, the indices used, and the vegetation type (Chen et al., 2002; Gilabert et al., 1996; Matsushita & Tamura, 2002; Qi et al., 2000). The common procedure was to establish an empirical relationship between a given spectral index and LAI by statistically fitting measured LAI values and corresponding values of that spectral index. In the current study, empirical relationships were determined from simulated data using PROSPECT and SAILH models. Predictive equations were developed for leaf chlorophyll concentrations varying from 20 to 100 μg cm^{-2} and LAI values ranging from 0.3 to 7. Best fits were obtained using exponential functions, with coefficients of determination (r^2) exceeding 0.98. Based on the analyses presented above, we have selected the following indices to estimate LAI from CASI hyperspectral images: RDVI, TVI, MSAVI, and MTVI2; selection criterion combines low sensitivity to chlorophyll content changes and sensitivity to LAI in crops with moderate to high density (LAI>3), as well as on the results of previous studies (Broge & Leblanc, 2000). Their predictive equations are as follows:

$$\text{RDVI:}\quad LAI = 0.0918\exp(6.0002\,RDVI)$$

$$\text{TVI:}\quad LAI = 0.1817\exp(4.1469\,TVI)$$

$$\text{MSAVI:}\quad LAI = 0.1663\exp(4.2731\,MSAVI)$$

$$\text{MTVI2:}\quad LAI = 0.2227\exp(3.6566\,MTVI2)$$

It is important to recall that these predictive equations were developed from simulated data, under specific conditions (Table 1): leaf dry matter content of 0.0035 g cm^{-2}, background reflectance of a developed soil, zenith angle of 45°, structural parameter N of 1.55, and a spherical LADF. Nevertheless, we have conducted other simulations with a structural parameter of 1.41, and a solar zenith angle of 35°, and found no difference in derived predictive equations. However, further simulations, and thorough analyses are required to assess the influence of these factors, the soil background, the atmosphere, and the LADF on prediction functions.

In analyses presented above, we have clearly demonstrated that modified variants of MCARI and TVI, developed as a part of this research, were the most suitable for LAI estimation from remote sensing data. First, they proved to be the less sensitive to leaf chlorophyll variations, which is the major factor that influences LAI retrieval from reflectance data. Second, they presented the best linear behavior with NIR reflectance extracted form CASI hyperspectral images, as well as with simulated LAI. Our calcu-

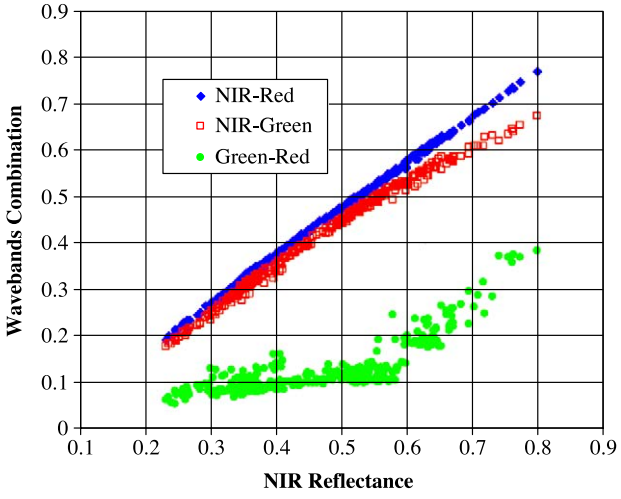

Fig. 5. Relationships between the near-infrared (NIR) reflectance and wavebands combinations, from CASI hyperspectral images collected over different crops (corn, wheat, and soybean). For clarity purposes, the difference Green – Red was multiplied by a factor of 4.

lations have shown that MTVI1 and MCARI1 have the disadvantage of overestimating green LAI. Consequently, they were not included among the indices selected for performance comparison in terms of predicting LAI. As for MCARI2, it was discarded because it has generated exactly the same results as MTVI2, owing to their similar mathematical forms.

3.4. Algorithms testing and validation: CASI data and ground truth

To test the above algorithms, we have used CASI hyperspectral images and corresponding ground truth measurements collected over different fields with various crops (soybean, corn, wheat) grown in different years (1999, 2000, 2001). Then, we have determined and assessed the accuracy of green LAI predictions given by the four indices RDVI, TVI, MSAVI, and MTVI2. Their predictive equations were applied to CASI images collected at different dates of the growing season in order to represent early vegetative, active, and reproductive growth stages. Then, mean values of estimated LAI were calculated for each crop type, for different nitrogen application rates, different drainage conditions, and for different growth stages captured in three intensive field campaigns. Comparisons with ground truth measurements using a combination of non-destructive and destructive LAI to extract green LAI (Table 2) were carried out, and corresponding results are presented in Figs. 6, 7, 8 and 10, and summarized in Table 3. For comparison purposes, for each crop, the predictions of the four indices were plotted against the ground truth on the same figure. As a preliminary assessment, figures and regression parameters (Table 3) show an excellent agreement between field measurements and resulting estimates of the algorithms using MSAVI and MTVI2 indices, with very consistent determination coefficients (r^2>0.90).

As shown in Fig. 6 and Table 3, MTVI2 and MSAVI predictions for soybean canopies have led to very high coefficients of determination (r^2>0.95), with root mean square errors (RMSE) less than 0.50, and correlation slopes close to one. As for RDVI and TVI, they have generated slope of 1.20 and 1.45, respectively, expressing an overestimation at high LAI levels (LAI>5) in comparison to observed LAI. It does not seem to be a measurement bias as both the destructive and non-destructive LAI values were within 0.5 at high LAI. Moreover, RDVI and TVI have resulted in higher RMSEs evaluated to 0.75 and 1.86, respectively.

In the case of corn canopies, we have found a very consistent agreement between LAI values measured in the field and those estimated by MTVI2 and MSAVI, with correlation slopes close to one, coefficients of determination (r^2) of 0.89 and 0.88, root mean square errors of 0.46 and 0.58, respectively (Fig. 7, Table 3). Independent data sets over corn fields from other locations in Canada were used to validate the algorithm; they led to similar results and were in

Table 2
Proportion of green LAI per crop and per intensive field campaigns (IFC) covering different periods of the 2001 growing season: map (1) = early growth stage (IFC1), map (2) = middle growth stage (IFC2), and map (3) = latest growth stage (maturity) (IFC3)

Crop	IFC1	IFC2	IFC3
Soybean	0.94–1.00	0.94–1.00	0.97–1.00
Corn	1.00	1.00	1.00
Wheat	0.97–1.00	0.90–0.99	0.40–0.84

Table 3
Characteristics of the regression between observed and estimated LAI values

Spectral index	Slope	Intercept	r^2	RMSE
Soybean				
MTVI2	1.010	+0.138	0.98	0.28
MSAVI	1.071	+0.040	0.97	0.43
RDVI	1.195	−0.061	0.95	0.75
TVI	1.445	−0.142	0.80	1.86
Corn				
MTVI2	1.027	+0.025	0.89	0.46
MSAVI	1.121	−0.050	0.88	0.58
RDVI	1.234	−0.124	0.90	0.66
TVI	1.444	−0.157	0.81	1.21
Wheat				
MTVI2	0.808	−0.166	0.74	0.85
MSAVI	0.873	−0.212	0.75	0.79
RDVI	0.998	−0.311	0.73	0.79
TVI	1.186	−0.391	0.56	1.28
Corn, soybean, and wheat				
MTVI2	1.046	+0.016	0.95	0.43
MSAVI	1.114	−0.040	0.93	0.55
RDVI	1.244	−0.132	0.93	0.76
TVI	1.501	−0.171	0.82	1.62

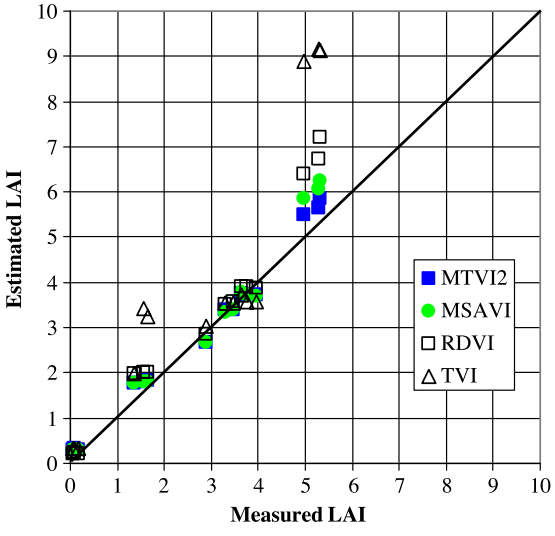

Fig. 6. Comparison between ground LAI measurements and green LAI estimations from CASI images using MTVI2, MSAVI, RDVI, and TVI, for soybean canopies.

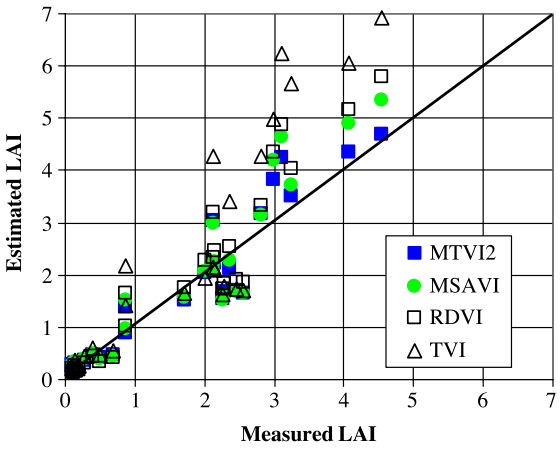

Fig. 7. Comparison between ground LAI measurements and green LAI estimations from CASI images using MTVI2, MSAVI, RDVI, and TVI, for corn canopies.

agreement with the expected inter-plot variability resulting from nitrogen and weed treatments; high nitrogen supply generated high values of LAI, while low nitrogen treatments produced lower LAI values. Moreover, MTVI2 estimates seem to be closer to the one-to-one line than MSAVI estimates. These results contrast with those of RDVI and TVI, which tend to overestimate the LAI in crop canopies with high density. This is corroborated by the values of their correlation slopes (1.21 and 1.41, respectively) and illustrated by their trend which diverts significantly from the one-to-one line (Fig. 7).

The results are quite different for wheat canopies. As can be seen in Fig. 8, the four indices behaved in two distinct ways: during the early vegetative stage (IFC1), MSAVI and MTVI2 have slightly followed the one-to-one line while RDVI and TVI have overestimated wheat canopy LAI; during the active growth and reproductive periods (IFC1 and IFC2), all indices have led to an underestimation of moderate to high LAI. Consequently, regression characteristics (Table 3) were consistent but less satisfactory: in comparison with corn and soybean canopies, indices have generated moderate to good coefficients of determination (ranging from 0.56 for TVI to 0.76 for MSAVI), low correlation slopes, and relatively high RMSE (0.79–1.28). According to our ground observation, the differences occurred at maturity (dominated by the heads of the wheat plant) and senescence stages (increase of yellow and dry leaves). In fact, while the approach for measuring non-destructive LAI using the LAI-2000 (Strachan et al., 2004) measures all light intercepting leaves of the plant (green and dead), our algorithm estimates only the green LAI due to photosynthetic elements of the plant (mainly green leaves). Indeed, the canopy reflectance modeling, with PROPSECT and SAILH, does not take into account the presence of stalks, heads, and senescent leaves.

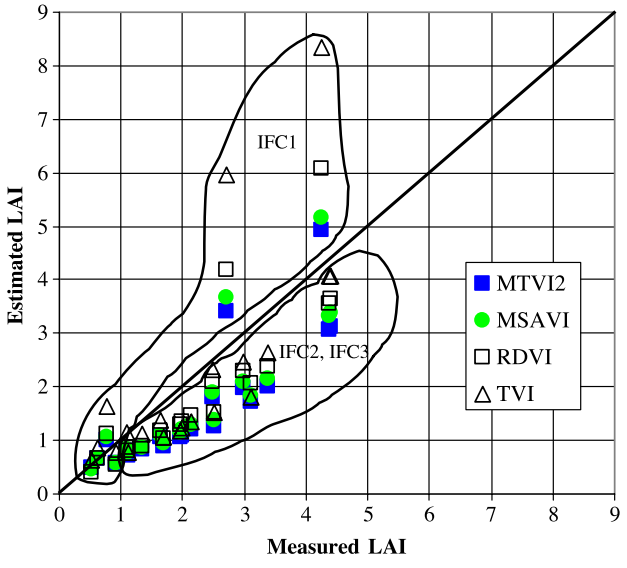

Fig. 8. Comparison between ground LAI measurements and green LAI estimations from CASI images using MTVI2, MSAVI, RDVI, and TVI for wheat canopies.

The effect of heads on wheat canopy reflectance is illustrated in Fig. 9, which shows spectra extracted from CASI hyperspectral images. They represent the same area of wheat field (sandy soil) at two different periods of the growing season: IFC1 corresponding to an active growth period dominated by green leaves, and IFC3 representing a reproductive canopy dominated by heads. It can be clearly seen that the presence of heads (and senescent leaves) induced a decrease in NIR reflectance, as well as a decrease of chlorophyll absorption (increase of red reflectance). Therefore, it has led to a reflectance spectrum that mimics a response of a canopy with low leaf area index, which explains the underestimation of LAI from hyperspectral images.

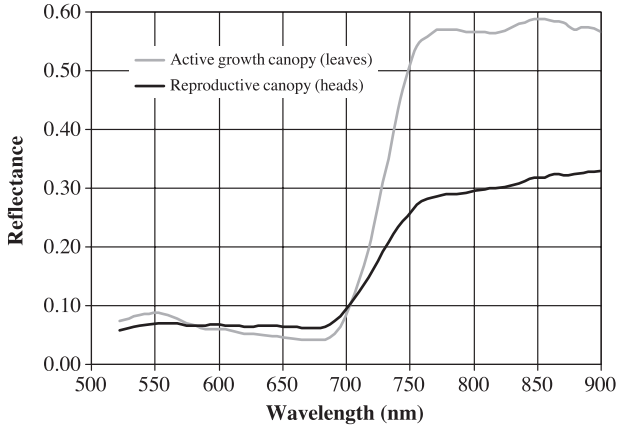

Fig. 9. Spectra of wheat canopies with dominating green leaves (active growth) and heads (reproductive period), extracted from CASI hyperspectral images over a sandy area at two different dates: IFC1 (active growth) and IFC3 (reproductive growth).

Finally, when soybean, corn, and wheat were considered together in the comparison between estimations and ground truth (Fig. 10), very good measures of the correlation were generated for MTVI2 and MSAVI: slopes close to one (1.05 and 1.11), excellent coefficients of determination (0.95 and 0.93), and reasonable RMSE (0.43 and 0.55). This significant result means that the proposed algorithm performs very well over various crop canopies having different leaf parameters, as well as different plant structures. These important findings were corroborated by MTVI2 and MSAVI algorithms testing on independent data sets obtained over corn and peas canopies grown in different locations in Quebec (Canada). Moreover, the data sets used in this study were appropriate for assessing the temporal evolution and the spatial variability of green LAI. Average values of LAI as low as 0.2 were estimated in early growth stages over plots with no nitrogen treatments, while average values as high as 5.35 and 6.25 were predicted at maximum growth for corn and soybean, respectively.

The analyses of the agreement between estimated and measured green LAI have resulted in excellent coefficients of determination (r^2) and excellent RMSE values for MTVI2 and MSAVI (Figs. 6, 7, 8 and 10; Table 3). In the case of wheat canopy, regressions do not follow exactly the one-to-one line, with slight biases expressed by non-zero intercepts. The problem of non-unity slope and intercept bias has been already reported in a study using models inversion to infer chlorophyll content of soybean canopies (Jacquemoud et al., 2000). It is not easy to single out a specific factor that could be responsible for such biases because a huge number of leaf and canopy descriptors were used in both reflectance modeling and scaling-up approach.

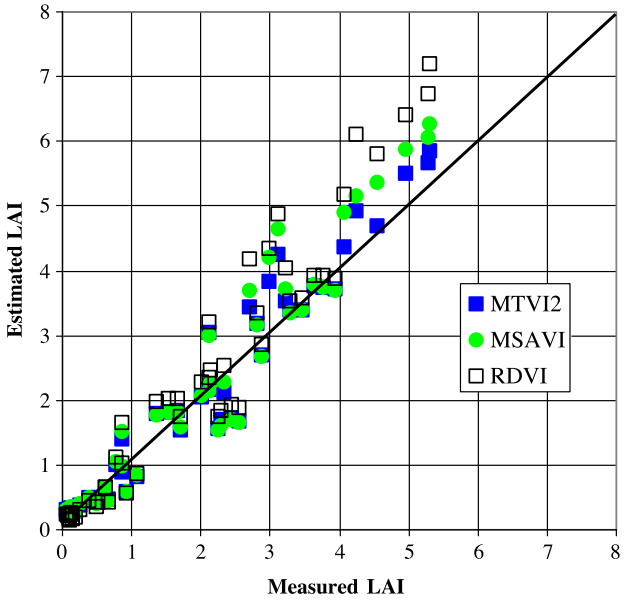

Fig. 10. Comparison between ground LAI measurements and green LAI estimations from CASI images using MTVI2, MSAVI, RDVI, and TVI, for soybean, corn, and wheat canopies.

Indeed, while the effect of each scale-dependent descriptor contributing to canopy reflectance is more or less well defined, the modeling and the scaling-up do not incorporate simultaneously the actual range of variation in plant characteristics and canopy structure that occur in the field.

The application of the MTVI2-based algorithm to CASI hyperspectral images, collected during the growing season of summer 2001, allowed the generation of maps of green LAI status of corn, wheat and soybean fields in terms of spatial variability and temporal changes. Fig. 11 represents green LAI maps corresponding to early (1), active (2), and reproductive (3) growth periods as observed in three intensive field campaigns (IFC1, IFC2, and IFC3). It clearly indicates the observed differences between crop types and phenological stages.

When the first CASI image was acquired (IFC1), the wheat crop was in the tillering phase with only a few advanced areas initiating the stem elongation phase. Observed LAI ranged from 1 to 4.3 (estimated LAI between 0.5 and 4.9). At the same time, the corn crop had 3–6 fully expanded leaves depending on the area (LAI < 0.2) and soybean had two fully expanded trifoliates (LAI < 0.2). The LAI variability within the wheat field is due in part to nitrogen supply and water availability and also to spring seeding conditions which influenced the dynamics of the canopy development. The high LAI levels observed in the northeastern portion (yellowish to reddish tones) of the wheat field are in an area with low clay which received the recommended nitrogen rate but was well drained following the wet spring enabling early and even emergence. The lowest LAI levels detected in the northwestern portion of the field (blue tones) result from topographic effects with a slope heading toward the creek flowing between the wheat and corn fields. The organic matter content was very low as a result of erosion occurring in this area. The southwestern square area (blue and cyan tones) of the field received only a starter rate of nitrogen, which generated a lag in the crop development. The diagonal strips (NW to SE) are filled water channels, which naturally provide water to the crop and thus are highly suitable for growth. The wheat field patterns identified in IFC1 were persistent through IFC3 and they are consistent with crop development. Indeed, the less productive areas showed increasing LAI over time, which indicated delays in the crop development, caused by the sub-optimum environmental growth conditions. The more productive areas exhibited decreasing LAI during IFC2 and 3 associated with heading, an indicator of a timely crop development associated with favorable environmental conditions (Fig. 11).

For both corn and soybean, LAI was continuously increasing from low levels (blue tones during IFC1) to very high levels (reddish and pink tones during IFC3). The corn canopy had a rapid leaf production between IFC2 and 3 growing from 6–9 fully expanded leaves to 8–13 fully expanded leaves with tassels emerged in productive zones. Observed and estimated green LAI were in the same range

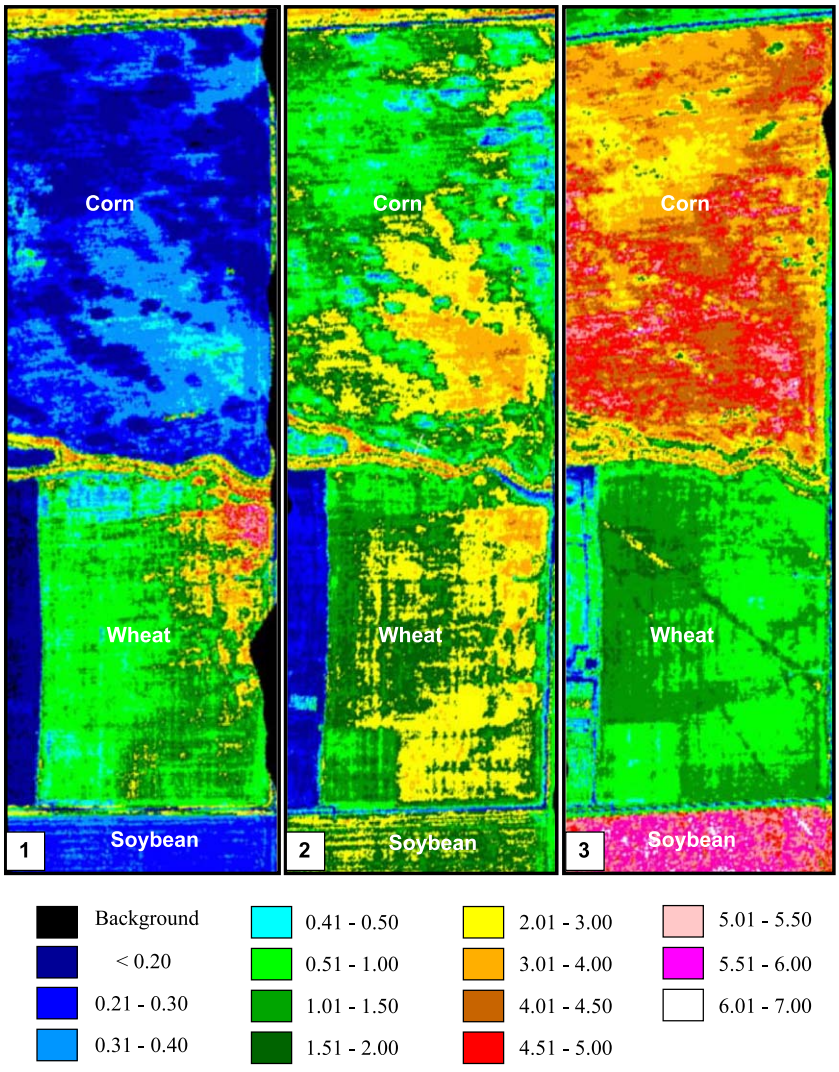

Fig. 11. Maps of green LAI determined with MTVI2-based algorithm from CASI hyperspectral images collected over the Former Greembelt Farm of Agriculture and Agri-Food Canada (Ottawa, Ontario, Canada). They represent three crops (corn in the northern portion, wheat in the middle, and soybean in the southern portion) observed in three intensive field campaigns (IFC) covering different periods of the 2001 growing season: map (1) = early growth stage (IFC1), map (2) = middle growth stage (IFC2), and map (3) = latest growth stage (maturity) (IFC3).

increasing from 0.1–0.4 in IFC1, to 1–3 in IFC2 and to 3–4.5 in IFC3 (Fig. 7). The area in IFC 3 with LAI>5 (light red and pink) had very high yield (data not shown), while the area with lower LAI (yellow) ended with below average yield, with identifiable patterns for both cases. The soybean canopy reached blooming onset in some areas during IFC2 and setting pods during IFC3. The soybean cultivar was indeterminate ideotype, which means that it continued to produce leaves during the reproductive phase. Estimated and observed green LAI were similar for IFC1 and IFC 2, but appeared slightly overestimated during IFC3 (Fig. 6). However, a wide range of LAI (4–7 m^2 m^{-2}) is estimated for IFC3, with a dense pattern of variation (Fig. 11). The high estimated green LAI values are in the range of values reported in the literature where maximum values are reported ranging from 6.5 to 9.0 depending on plant densities (Pengelly et al., 1999). Each IFC covered a wide span of green LAI with flight lines encompassing three different field crops. This wide range of LAI was verified by detailed ground-truth observations obtained within contrasting productivity areas.

4. Conclusions

Quantification of the canopy leaf area index (LAI) and its spatial distribution provides an avenue to improve the interpretation of remotely sensed data over vegetated areas, as well as valuable information to aid the development of approaches for ecosystem functioning and ecosystem productivity. Due to the complexity of the relationship between canopy reflectance and its biochemical components and structural descriptors, the present study used the radiative transfer model, PROSPECT and SAILH, to simulate crop

canopy reflectance for a wide range of both pigments and LAI. This simulation study was carried out to test existing vegetation indices, as well as new spectral indices developed as a part of this research, for green LAI prediction from remotely sensed data. It allowed us to compare, on a consistent basis, the performance of a set of indices both in terms of their resistance to chlorophyll effects, and the linearity of their relationships with green LAI. New spectral indices (MTVI2, MCARI2) and corresponding novel LAI prediction algorithms were developed, and validated on CASI hyperspectral data sets collected during several intensive field campaigns, over various crops, in three different years. As a result of thorough analyses of both simulations and applications to real hyperspectral data, the following conclusions are drawn.

Overall, the most robust indices are MTVI2 and MCARI2, which were developed in the context of this study as best estimators of green LAI. They are modified and improved variants of spectral indices initially designed to measure photosynthetically active radiation related to chlorophyll absorption (TVI and MCARI). Simulated data have shown that MCARI2 and MTVI2 were less sensitive to chlorophyll concentration variations, have the best linear relationship with near-infrared canopy reflectance, and therefore, the best linearity with green LAI.

Based on the performances of these two indices, new algorithms were proposed to predict green LAI of crop canopies. These novel algorithms are developed from modeling and scaling-up approaches using the leaf and canopy radiative transfer models PROSPECT and SAILH, respectively. These algorithms were successfully tested with airborne CASI hyperspectral images acquired over fields of corn, soybean, and wheat and then validated using ground truth data collected simultaneously to images acquired at the early, mid-, and late growth stages of each of the crops. Excellent agreements were found between modeled and measured LAI, with very high determination coefficients (r^2), and very good mean root square (RMSE) estimates. r^2 values were determined as 0.98 for soybean, 0.89 for corn, and 0.74 for wheat, and with corresponding RMSE of 0.28, 0.46, and 0.85, respectively.

Analysis based on simulated and real hyperspectral data showed significantly greater saturation problems in the relationships between LAI and some indices like NDVI and MSR. In addition, the latter suffer significantly from the strong influence of chlorophyll content variations. Other indices such as MSAVI, SAVI, and SARVI exhibited better performances, but they were still affected by changes at moderate chlorophyll levels, and tended to noticeable saturation for high LAI levels. Conversely, MTVI1 and MCARI1 presented a similar behavior as their equivalents MTVI2 and MCARI2, but tended to be extremely influenced by NIR reflectance variations, leading therefore to an overestimation of LAI.

Algorithms to predict LAI proposed in this article, together with ground truth data, have pointed out some limiting factors related to canopy reflectance modeling with PROPSECT and SAILH; namely, the presence of heads in the wheat field, and the effect of senescent and dry vegetation. The fact that these canopy components were not taken into account resulted in an underestimation of total LAI which could in turn affect estimates of biomass, carbon assimilation, etc. Therefore, correlation coefficients and prediction accuracy should be interpreted with caution, as well as with regards to the specific variable the indices were designed to measure—in this case, green LAI associated with living leaves.

Nevertheless, one of the main conclusions of this study is the important role of modeling based on PROSPECT and SAILH in developing and testing various spectral indices, as well as understanding the effect that key vegetation biochemical and structural parameters have on canopy reflectance. Moreover, these models were essential to the development of predictive algorithms that could not be efficiently designed from measurements and observations in the field and/or laboratory. Such an approach of algorithm development from purely simulated data, together with its successful application to real remotely sensed data holds a strong potential for operational quantification of vegetation variables such as LAI and chlorophyll content. This is of major importance for precision agriculture, and potentially, for other vegetated environments.

Acknowledgements

The authors are very grateful for the financial support provided by GEOmatics for Informed Decisions (GEOIDE), the Canadian Space Agency (CSA) and Agriculture and Agri-Food Canada. We thank Lawrence Gray, Phil Brasher and Heidi Beck of Aviation International for making CASI airborne field campaigns work efficiently. The field support of Lynda Blackburn, Dave Dow, Mathew Hinther and Dave Meridith was greatly appreciated. We also thank anonymous reviewers for valuable suggestions and criticism. ECORC contribution number: 03-12345.

References

Bannari, A., Huete, A. R., Morin, D., & Zagolski, F. (1996). Effets de la couleur et de la brillance du sol sur les indices de végétation. *Int. J. Remote Sens.*, *17*, 1885–1906.

Bannari, A., Morin, D., Bonn, F., & Huete, A. R. (1995). A review of vegetation indices. *Remote Sens. Rev.*, *13*, 95–120.

Baret, F., & Guyot, G. (1991). Potentials and limits of vegetation indices for LAI and APAR assessment. *Remote Sens. Environ.*, *35*, 161–173.

Baret, F., Guyot, G., & Major, D. J. (1989). TSAVI: A vegetation index which minimizes soil brightness effects on LAI and APAR estimation. *Proc. IGARSS'89 and 12th Canadian Symposium on Remote Sensing, Vancouver, Canada* (pp. 1355–1358).

Broge, N. H., & Leblanc, E. (2000). Comparing prediction power and stability of broadband and hyperspectral vegetation indices for estimation of green leaf area index and canopy chlorophyll density. *Remote Sens. Environ.*, *76*, 156–172.

Brown, L., Jin, M. C., Lablanc, S. G., & Cihlar, J. (2000). A shortwave infrared modification to the simple ratio for LAI retrieval in boreal forests: An image and model analysis. *Remote Sens. Environ.*, *71*, 16–25.

Chappelle, E. W., Kim, M. S., & McMurtrey III, J. E. (1992). Ratio analysis of reflectance spectra (RARS): An algorithm for the remote estimation of the concentrations of chlorophyll a, chlorophyll b, and the carotenoids in soybean leaves. *Remote Sens. Environ.*, *39*, 239–247.

Chen, J. (1996). Evaluation of vegetation indices and modified simple ratio for boreal applications. *Can. J. Remote Sens.*, *22*, 229–242.

Chen, J., & Cihlar, J. (1996). Retrieving leaf area index of boreal conifer forests using Landsat Thematic Mapper. *Remote Sens. Environ.*, *55*, 153–162.

Chen, J., Pavlic, G., Brown, L., Cihlar, J., Leblanc, S. G., White, P. H., Hall, R. J., Peddle, D. R., King, D. J., Trofymow, J. A., Swift, E., Van der Sanden, J., & Pellikka, P. K. E. (2002). Derivation and validation of Canada-wide coarse-resolution leaf area index maps using high-resolution satellite imagery and ground measurements. *Remote Sens. Environ.*, *55*, 153–162.

Daughtry, C. S. T., Gallo, K. P., Goward, S. N., Prince, S. D., & Kustas, W. D. (1992). Spectral estimates of absorbed radiation and phytomass production in corn and soybean canopies. *Remote Sens. Environ.*, *39*, 141–152.

Daughtry, C. S. T., Walthall, C. L., Kim, M. S., Brown de Colstoun, E., & McMurtrey III, J. E. (2000). Estimating corn leaf chlorophyll concentration from leaf and canopy reflectance. *Remote Sens. Environ.*, *74*, 229–239.

Fassnacht, K. S., Gower, S. T., MacKenzie, M. D., Nordheim, E. V., & Lillesand, T. M. (1997). Estimating the leaf area index of north central Wisconsin forest using Landsat Thematic Mapper. *Remote Sens. Environ.*, *61*, 229–245.

Gamon, J. A., Penuelas, J., & Field, C. B. (1992). A narrow-waveband spectral index that tracks diurnal changes in photosynthetic efficiency. *Remote Sens. Environ.*, *41*, 35–44.

Gilabert, M. A., Gandia, S., & Melia, J. (1996). Analyses of spectral–biophysical relationships for a corn canopy. *Remote Sens. Environ.*, *55*, 11–20.

Gitelson, A., Rundquist, D., Derry, D., Ramirez, J., Keydan, G., Stark, R., & Perk, R. (2001). Using remote sensing to quantify vegetation fraction in corn canopies. *Proc. Third Conference on Geospatial Information in Agriculture and Forestry, Denver, Colorado, 3–7 November 2001*.

Gitelson, A. A., & Merzlyak, M. N. (1996). Signature analysis of leaf reflectance spectra: Algorithm development for remote sensing. *J. Plant Physiol.*, *148*, 493–500.

Goel, N. S. (1988). Models of vegetation canopy reflectance and their use in estimation of biophysical parameters from reflectance data. *Remote Sens. Rev.*, *4*, 1–212.

Goel, N. S. (1989). Inversion of canopy reflectance models for estimation of biophysical parameters from reflectance data. In G. Asrar (Ed.), *Theory and applications of optical remote sensing* (pp. 205–251). New York: Wiley.

Goetz, S. J., & Prince, S. D. (1996). Remote sensing of net primary production in boreal forest stands. *Agric. For. Ecol.*, *78*, 149–179.

Govaerts, Y. M., Verstraete, M. M., Pinty, B., & Gobron, N. (1999). Designing optimal spectral indices: A feasibility and proof of concept study. *Int. J. Remote Sens.*, *20*, 1853–1873.

Haboudane, D., Miller, J. R., Tremblay, N., Zarco-Tejada, P. J., & Dextraze, L. (2002). Integrated narrow-band vegetation indices for prediction of crop chlorophyll content for application to precision agriculture. *Remote Sens. Environ.*, *81*, 416–426.

Hu, B., Miller, J. R., Chen, J. M., & Hollinger, A. B. (2004). Retrieval of the canopy leaf area index in the BOREAS flux tower sites using linear spectral mixture analysis. *Remote Sens. Environ.*, *89*, 176–188.

Huete, A. R. (1988). A soil vegetation adjusted index (SAVI). *Remote Sens. Environ.*, *25*, 295–309.

Jacquemoud, S., & Baret, F. (1990). Prospect: A model for leaf optical properties spectra. *Remote Sens. Environ.*, *34*, 75–91.

Jacquemoud, S., Bacour, C., Poilve, H., & Frangi, J. -P. (2000). Comparison of four radiative transfer models to simulate plant canopies reflectance: Direct and inverse mode. *Remote Sens. Environ.*, *74*, 417–481.

Jacquemoud, S., Ustin, S. L., Verdebout, J., Schmuck, G., Andreoli, G., & Hosgood, B. (1996). Estimating leaf biochemistry using the PROSPECT leaf optical properties model. *Remote Sens. Environ.*, *56*, 194–202.

Jordan, C. F. (1969). Derivation of leaf area index from quality of light on the forest floor. *Ecology*, *50*, 663–666.

Karnieli, A., Kaufman, Y. J., Remer, L., & Wald, A. (2001). AFRI—aerosol free vegetation index. *Remote Sens. Environ.*, *77*, 10–21.

Kaufman, Y. J., & Tanre, D. (1992). Atmospherically resistant vegetation index (ARVI). *IEEE Trans. Geosci. Remote Sens.*, *30*, 261–270.

Kim, M. S., Daughtry, C. S. T., Chappelle, E. W., McMurtrey III, J. E., & Walthall, C. L. (1994). The use of high spectral resolution bands for estimating absorbed photosynthetically active radiation (Apar). *Proceedings of the 6th Symp. on Physical Measurements and Signatures in Remote Sensing, Jan. 17–21, 1994, Val D'Isere, France* (pp. 299–306).

Kuusk, A. (1985). The hot spot effect on a uniform vegetative cover. *Sov. J. Remote Sens.*, *3*, 645–658.

Lillesaeter, O. (1982). Spectral reflectance of partly transmitting leaves: Laboratory measurements and mathematical modeling. *Remote Sens. Environ.*, *12*, 247–254.

Liu, J., Chen, J., Cihlar, J., & Park, W. M. (1997). A process-based boreal ecosystem productivity simulator using remote sensing inputs. *Remote Sens. Environ.*, *62*, 158–175.

Matsushita, B., & Tamura, M. (2002). Integrating remotely sensed data with an ecosystem model to estimate net primary productivity in East Asia. *Remote Sens. Environ.*, *81*, 58–66.

Moran, M. S., Inoue, Y., & Barnes, E. M. (1997). Opportunities and limitations for image-based remote sensing in precision crop management. *Remote Sens. Environ.*, *61*, 319–346.

Moran, M. S., Maas, S. J., & Pinter Jr., P. J. (1995). Combining remote sensing and modeling for estimating surface evaporation and biomass production. *Remote Sens. Environ.*, *12*, 335–353.

Nemani, R., Pierce, L., Running, S., & Band, L. (1993). Forest ecosystem processes at the watershed scale: Sensitivity to remotely-sensed leaf area index estimates. *Int. J. Remote Sens.*, *14*, 2519–2534.

O'Neill, N. T., Zagolski, F., Bergeron, M., Royer, A., Miller, R. J., & Freemantle, J. (1997). Atmospheric correction validation of CASI images acquired over the BOREAS southern study area. *Can. J. Remote Sens.*, *23*, 143–162.

Pacheco, A., Bannari, A., Deguise, J. -C., McNairn, H., & Staenz, K. (2001). Application of hyperspectral remote sensing for LAI estimation in Precision Farming. *23rd Canadian Symposium on Remote Sensing—10e Congres de l'Association Quebecoise de Teledetection, Quebec City, Canada, 21–25 August 2001*.

Pattey, E., Strachan, I. B., Boisvert, J. B., Desjardins, R. L., & McLaughlin, N. (2001). Effects of nitrogen application rate and weather on corn using micrometeorological and hyperspectral reflectance measurements. *Agric. For. Meteorol.*, *108*, 85–99.

Peddle, D. R., & Johnson, R. L. (2000). Spectral mixture analysis of airborne remote sensing imagery for improved prediction of leaf area index in Mountainous Terrain, Kananaskis, Alberta. *Can. J. Remote Sens.*, *26*, 176–187.

Pengelly, B. C., Blamey, F. P. C., & Muchow, R. C. (1999). Radiation interception and the accumulation of biomass and nitrogen by soybean and three tropical annual forage legumes. *Field Crops Res.*, *63*, 99–112.

Qi, J., Chehbouni, A., Huete, A. R., Keer, Y. H., & Sorooshian, S. (1994). A modified soil vegetation adjusted index. *Remote Sens. Environ.*, *48*, 119–126.

Qi, J., Kerr, Y. H., Moran, M. S., Weltz, M., Huete, A. R., Sorooshian, S., & Bryant, R. (2000). Leaf area index estimates using remotely sensed data and BRDF models in a semiarid region. *Remote Sens. Environ.*, *73*, 18–30.

Rondeaux, G., Steven, M., & Baret, F. (1996). Optimization of soil-adjusted vegetation indices. *Remote Sens. Environ.*, *55*, 95–107.

Rougean, J. -L., & Breon, F. M. (1995). Estimating PAR absorbed by

vegetation from bidirectional reflectance measurements. *Remote Sens. Environ.*, *51*, 375–384.

Rouse, J. W., Haas, R. H., Schell, J. A., Deering, D. W., & Harlan, J. C. (1974). Monitoring the vernal advancements and retrogradation of natural vegetation. In: *NASA/GSFC, Final Report, Greenbelt, MD, USA* (pp. 1–137).

Spanner, M. A., Pierce, L. L., Peterson, D. L., & Running, S. W. (1990). Remote sensing of temperate coniferous forest leaf area index. The influence of canopy closure, understory vegetation and background reflectance. *Int. J. Remote Sens.*, *11*, 95–111.

Strachan, I. B., Pattey, E., & Boisvert, J. B. (2002). Impact of nitrogen and environmental conditions on corn as detected by hyperspectral reflectance. *Remote Sens. Environ.*, *80*, 213–224.

Strachan, I. B., Stewart, D. W., & Pattey, E. (2004). Leaf area index. *ASA Monograph* (in press, Book Chapter).

Tucker, C. J., Holben, B. N., Elgin Jr., J. H., & McMurtrey, J. E. (1980). Relationship of spectral data to grain yield variations. *Photogramm. Eng. Remote. Sens.*, *46*, 657–666.

Verhoef, W. (1984). Light scattering by leaf layers with application to canopy reflectance modeling: The SAIL model. *Remote Sens. Environ.*, *16*, 125–141.

Verhoef, W. (1998). *Theory of radiative transfer models applied in optical remote sensing of vegetation canopies*. Wageningen: Grafish Service Centrum Van Gils.

Zarco-Tejada, P. J. (2000). Hyperspectral remote sensing of closed forest canopies: Estimation of chlorophyll fluorescence and pigment content. *PhD thesis, Graduate programme in Earth and Space Science, York University, Toronto, Ontario, Canada* (p. 210).

Zarco-Tejada, P. J., Miller, J. R., Noland, T. L., Mohammed, G. H., & Sampson, P. H. (2001). Scaling-up and model inversion methods with narrow-band optical indices for chlorophyll content estimation in closed forest canopies with hyperspectral data. *IEEE Trans. Geosci. Remote Sens.*, *39*(7), 1491–1507.